Spin Seebeck Effect in Fe/Co and Co/Pt layers of Thin Films Using First Principle and Experimental Setup

Pirapat Waritkraikul[1], Santi Phumying[4], Annop Ektarawong[2], Wutthikrai Busayaporn[3], Poramed Wongjom[4], and Wanchai Pijitrojana[1,*]

[1]Electrical and Computer Engineering Department, Thammasat School of Engineering, Thammasat University, Rangsit Campus, Klongluang, Pathumthani 12120 Thailand.
[2]Extreme Conditions Physics Research Laboratory and Center of Excellence in Physics of Energy Materials, Department of Physics, Faculty of Science, Chulalongkorn University, Bangkok 10330, Thailand.
[3]Synchrotron Light Research Institute (Public Organization), Nakhon Ratchasima 30000, Thailand.
[4]Division of Physics, Faculty of Science and Technology, Thammasat University, Pathum Thani 12120, Thailand.

Abstract: This research is focusing to examining the electronic structure and electrical properties of the Fe/Co and Co/Pt systems in comparison with the Fe/Pt system through the use of Density Functional Theory (DFT). The results indicate that the Fe/Co and Co/Pt systems exhibit significantly less electrical mismatch than the Fe/Pt system, as evidenced by a broader distribution of the Total Density of States (TDOS) near the Fermi energy level. Further analysis of the Projected Density of States (PDOS) for the d orbitals of Fe and Co in the Fe/Co system, and of Co and Pt in the Co/Pt system, confirms that the predominant characteristics of both systems are driven by the influence of d orbitals. This insight is critical for the selection of materials for the investigation of the Spin Seebeck Effect (SSE), particularly in understanding the electrical conductivity and magnetic properties of the materials of interest prior to experimental trials. This study deepens the understanding of the relationship between electronic structure and the electrical and magnetic properties of materials, which is vital for the design and application of materials in spintronics technology, especially in studying the Spin Seebeck Effect. This phenomenon involves the conversion of thermal energy into electrical energy using the spin of electrons.

***Keywords*—Density Functional Theory (DFT), Spin Seebeck Effect, Spintronics.**

I. Introduction

The Spin Seebeck Effect (SSE) has garnered substantial interest within the field of spintronics, examining the interplay between charge, spin, and thermal energies. This phenomenon is rooted in the Seebeck Effect, which describes the generation of an electromotive force (EMF) across two points of a material or between different materials subjected to a thermal gradient. When materials at varying temperatures are connected, the movement of electrons induces an EMF, allowing for the measurement of electrical voltage across two points. The SSE pertains to the generation of a spin current induced by a thermal gradient in ferromagnetic materials (FM), facilitating the injection of spin currents from ferromagnetic materials into nonmagnetic materials or metals. This process leverages the Inverse Spin Hall Effect (ISHE), where the injected spin current is converted into a transverse charge voltage without the direct movement of electrical charges. This mechanism is crucial for detecting and converting spin signals into measurable electrical signals in electronic devices. These discoveries unveil the mechanisms behind the SSE and propose new applications in spintronics technologies. Further studies on magnons and phonons enhance understanding of how thermal energy can be converted into spin currents, leading to the generation of electromotive forces. Advances in this area could lead to the development of new materials and devices with improved energy conversion efficiency and

The manuscript received May 27, 2024; revised June 15, 2024; accepted June 25, 2024; Date of publication June 30, 2024
*Correspondence: Wanchai Pijitrojana, Electrical and Computer Engineering Department, Thammasat School of Engineering, Thammasat University, Rangsit Campus, Klongluang, Pathum Thani 12120 Thailand, (E-mail: pwanchai@engr.tu.ac.th)

broader applications in the future [1-5].

Current research extensively investigates the Spin Seebeck Effect (SSE), with experimental studies focusing on specific materials such as the magnetic insulator Yttrium Iron Garnet (YIG) and the non-magnetic metal platinum (Pt). YIG, as a magnetic insulator, exhibits favorable characteristics for generating and maintaining spin states, rendering it an ideal material for spin current studies. Conversely, platinum (Pt) , lacking magnetic properties, effectively detects spin currents generated by YIG upon thermal excitation. The synergy between these two materials enhances the understanding and exploration of the Spin Seebeck Effect, facilitating a more comprehensive study of spin currents and their applications in spintronics.

To elucidate the Spin Seebeck Effect (SSE) , Density Functional Theory (DFT) serves as a crucial theoretical tool in the study of materials and molecules within the fields of chemistry and physics, offering a deeper understanding of electronic structures and magnetic properties [6] . An important aspect of DFT calculations is the creation of material surfaces for use in simulations, which involves modeling the surfaces to closely resemble reality. This is best achieved by slicing the crystal in the desired direction for study. The application of DFT in investigating the SSE allows for the analysis of electronic structures and identifies magnons and phonons as significant factors influencing the performance of SSE.

Yttrium Iron Garnet (YIG) is identified as a ferrimagnetic material with the chemical formula $Y_3Fe_5O_{12}$. In this structure, yttrium (Y) atoms do not exhibit magnetic properties, whereas iron (Fe) atoms contribute to the material's magnetic characteristics. It is worth noting that most of the magnetic moment in the unit cell of YIG is widely distributed among the iron (Fe) atoms. This indicates that the magnetic properties of YIG are predominantly determined by its iron (Fe) atoms [7]. This research focuses on studying the structures of iron (Fe) combined with cobalt (Co) , and cobalt (Co) with platinum (Pt) through Density Functional Theory calculations. The results from the first principle of this research is also to confirm and compare to the results of the experiments in [8]. The process begins with the simulation of the crystal structures of the three materials, including iron (Fe) , cobalt (Co) , and platinum (Pt) . Subsequently, density functional theory calculations are performed using the VASP (Vienna Ab initio Simulation Package) software, followed by an analysis of the results.

II. Computational Methods

First-principles calculations are performed using the density functional theory (DFT) framework, as facilitated by the Vienna Ab initio Simulation Package (VASP). The methodology employs spin-polarized Projector Augmented-Wave (PAW) pseudopotentials with a designated kinetic energy cutoff of 520 eV. Exchange-correlation interactions are managed through the Perdew-Burke-Ernzerhof (PBE) generalized gradient approximation (GGA). In the setup, a layer of iron (Fe) consisting of five body-centered cubic (bcc) Fe (110) monolayers, a layer of cobalt (Co) comprising five hexagonal close-packed (hcp) Co ($11\bar{2}0$) monolayers, and a layer of platinum (Pt) made up of five face-centered cubic (fcc) Pt (110) monolayers are constructed. The total assembly for the Fe/Co interface includes 20 atoms, evenly split between 10 Fe and 10 Co atoms, and similarly, the Co/Pt interface encompasses 20 atoms, with an equal division of 10 Co and 10 Pt atoms. A 20 Å vacuum layer is introduced along the z-axis to prevent interactions with neighboring unit cells, while a 7 x 7 x 1 Monkhorst-Pack grid is employed to systematically sample the reciprocal space. Within the Fe/Co and Co/Pt structures, the interfacial layers directly adjoining Fe and Co, and Co and Pt, respectively, are immobilized during the process of relaxation. Relaxation is allowed for all other atoms until the energy shift is less than 10^{-6} eV, and the forces on the atoms decrease to below 0.02 eV/Å.

III. Results and Discussion

The transport properties are predominantly determined by the electron state density at the Fermi energy level (EF). Research [7] has revealed that for the Fe/Pt structure, the spin-polarized total density of states (TDOS) near the Fermi energy level predominantly arises from minority spins (spin down). This study's density functional theory (DFT) calculations indicate that at the Fermi energy level, the spin-polarized total density of states in the Fe/Co structure system, as shown in Figure 1, displays closely matched values for both spin-up and spin-down states. Furthermore, the total density of state density near the Fermi level for the Fe/Co system, as depicted in Figure 2, exhibits a larger dispersion of total density of states compared to the Fe/Pt system [7]. This suggests a favorable tendency of the Fe/Co structure system over the Fe/Pt structure system in terms of electrical mismatch, attributed to the interface between iron (Fe) and cobalt (Co). Similarly, for the Co/Pt structure system, the total density of states near the Fermi energy level, shown in Figure 4, exhibits a larger dispersion of total density of states compared to the Fe/Pt structure system [7]. This is a result of the interface between cobalt (Co) and platinum (Pt), according to the outcomes of the density functional theory calculations.

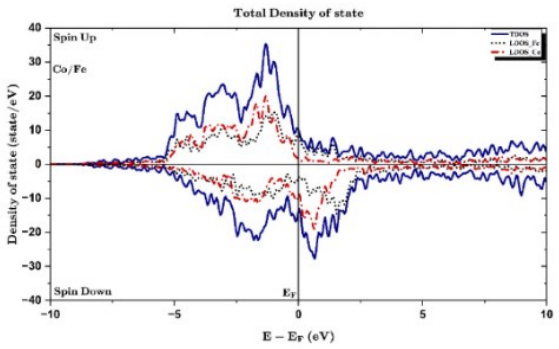

Fig. 1 Spin-polarized TDOS for the Fe and Co layers (Fe/Co)

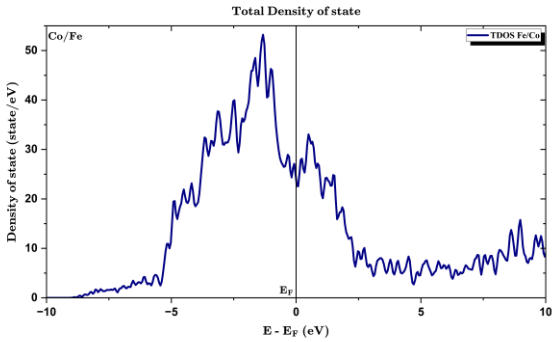

Fig. 2 TDOS for the Fe and Co layers (Fe/Co)

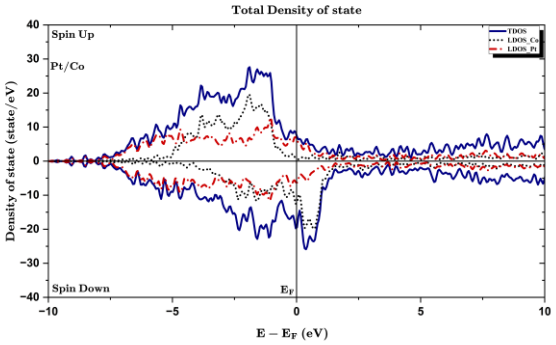

Fig. 3 Spin-polarized TDOS for the Co and Pt layers (Co/Pt)

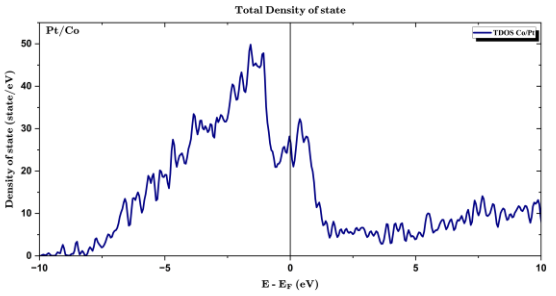

Fig. 4 TDOS for the Co and Pt layers (Co/Pt)

From the results of the Projected Density of States (PDOS) for the Fe/Co system, the partial electron density states from the s, p, and d orbitals for both iron (Fe), as illustrated in Figure 5, and cobalt (Co), as depicted in Figure 6, it can be seen that the Total Density of States (TDOS) primarily arises from the d orbitals. Therefore, the magnetic and electrical properties of the Fe/Co structure predominantly originate from d orbitals. Similarly, for the Co/Pt system structure, the partial electron density states from the s, p, d, and f orbitals, as shown in Figures 7 and 8, suggest that the various properties of the Co/Pt structure are also mainly derived from d orbitals.

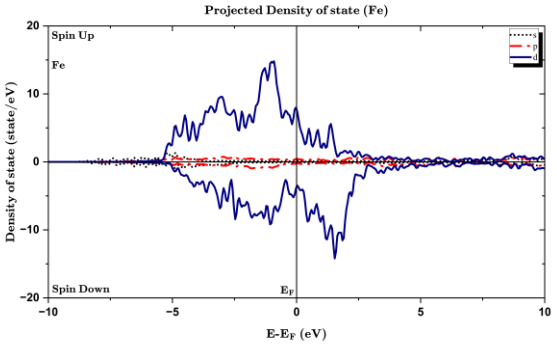

Fig. 5 Spin-polarized PDOS for Fe layers from Fe/Co structure

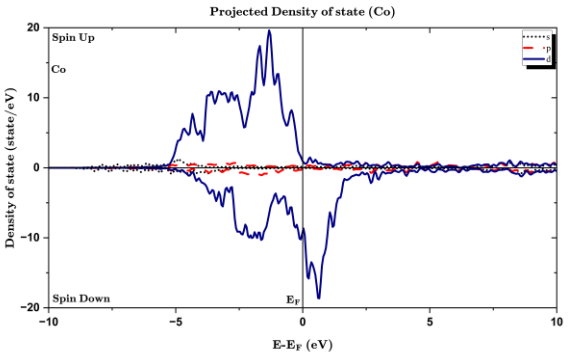

Fig. 6 Spin-polarized PDOS for Co layers from Fe/Co structure

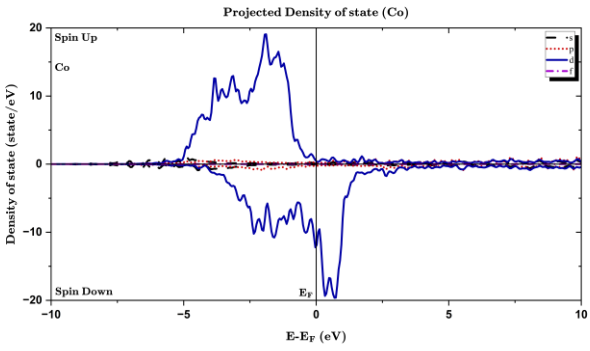

Fig. 7 Spin-polarized PDOS for Co layers from Co/Pt structure

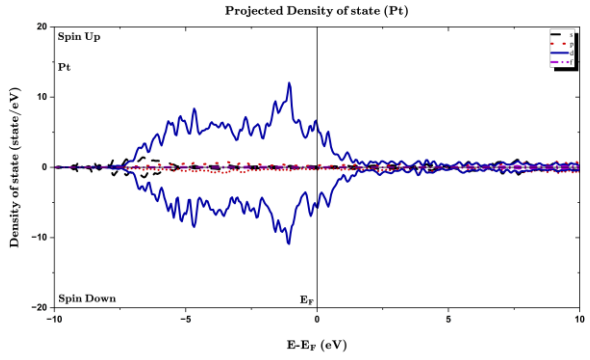

Fig. 8 Spin-polarized PDOS for Pt layers from Co/Pt structure

TABLE I
SPIN POLARIZED TOTAL DENSITY OF STATES AT THE FERMI ENERGY LEVEL $N(E_F)$ (STATES/EV) OF THE FE/CO AND CO/PT STRUCTURE

Material	Spin polarized TDOS at the Fermi energy level (states/eV)		
	Spin (↑)	Spin (↓)	Total
Fe/Co	9.487	13.14	22.627
Co/Pt	7.13	19.42	26.55

To compare the calculation results with the experimental results, we fabricated the Iron (Fe) and Cobalt (Co) film on a Si-wafer substrate (Si/Fe 500nm/Co-10nm) [8]. Fig. 9a shows the spin Seebeck Effect setup (sample).

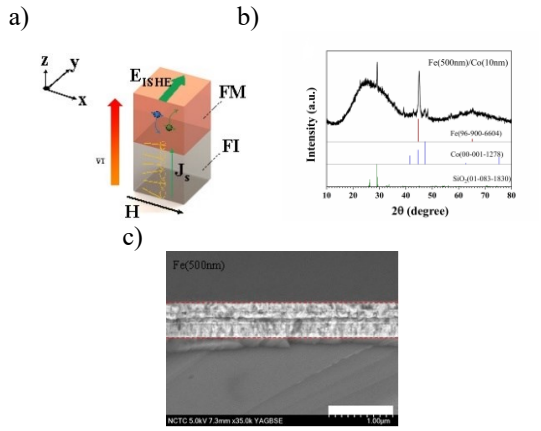

Fig.9 a) SSE setup, the magnetic field (***H***) and temperature gradient (***∇T***) are applied to sample in x-axis and z-axis, respectively. The voltage is observed in y-axis b) The x-ray diffraction (XRD) pattern of Fe(500nm)/Co(10nm) c) The scanning electron microscope (SEM) image of side view of Fe(500nm)

The morphology phase diagram of Fe, Co and Fe/Co is shown in Fig.9b which is illustrated polycrystalline materials and corresponded to 96-900-6604 and 00-001-1278 database. The thicknesses of Fe and Co film are 500 nm and 10 nm, respectively as shown in Fig.9c. The coercive force (Hc) of Fe, Fe/Co and Co are 30.53 Oe (-67.07 Oe), 30,53 Oe (-42.53) and 82.15 Oe (-67.07 Oe), respectively, while the magnetic saturation (Ms) of Fe, Fe/Co and Co are $1.25x10^6$ emu/m^3 (at H=400 Oe), $1.5x10^6$ emu/m^3 (at H=341 Oe) and $1.08x10^4$ emu/m^3 (at H=479 Oe), respectively which is shown in Fig.10. As seen the Ms of magnetic thin film, the magnetic moment (μ) of Fe film is larger than Co film about 2 orders which the Fe film is dominants to Fe/Co structure.

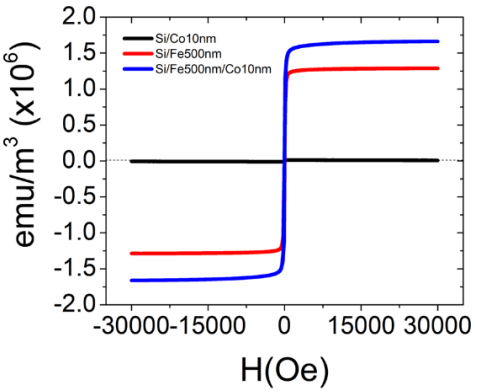

Fig. 10 Vibration sample microscopy (VSM) of Co10nm, Fe500nm and Fe500nm/Co10nm

For observation the SSE, the longitudinal spin Seebeck effect (LSSE) is used to detect the phenomena which the spin injection (J_s) is parallel to temperature gradient (***∇T***) as seen in Fig.9a. The Fe, Co and Fe/Co films are applied magnetic field strength (***H***) in x-axis and the temperature gradient (***∇T***) in z-axis, while the voltage is also detected in y-axis. For temperature dependent, the magnetic field of Fe and Fe/Co film is fixed at 1,500 Oe field strength, while the voltage detection is linearly increasing as shown in Fig.11a and Fig.11c. But the voltage on Co film is tending to linearly decrease with temperature gradient (***∇T***) increment. Because the spin Hall angle (θ_H) of Fe and Co is opposite, the electric field or voltage conversion are also opposite as correspond to Bavontaweepanya R. [9]. The voltage conversion [(electric field (***E***)/temperature gradient (***∇T***)] which is comparing to temperature difference of Fe, Co and Fe/Co is 0.012 µV/K, -0.078 µV/K and 0.009 µV/K, respectively.

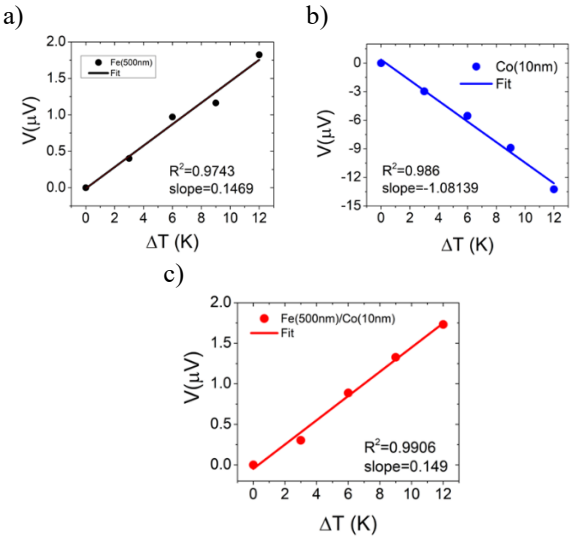

Fig.11 The temperature gradient ***(∇T)*** dependence
a) Fe*(500nm)* ***b)*** Co*(10nm)* ***c)*** Fe*(500nm)*/Co*(10nm)*

The Fig.12 is shown the magnetic field dependence of Fe, Co and Fe/Co, respectively. Note again that the signal of Fe and Co film is opposite direction. However, when LSSE configuration is used to observed SSE, the spin injector is needed to be FI materials. Here, we used Fe film which is FM material as spin injector and coated with Co film. We found that the voltage signal of Fe/Co film is similar behavior to Fe film as seen in Fig.12c. So, we have compared voltage signal between Fe and Fe/Co film. We found that the magnitudes of voltage in Fe and Fe/Co film are 12.28 nV/K and 8.8 nV/K, respectively as illustrated in Fig.12d.

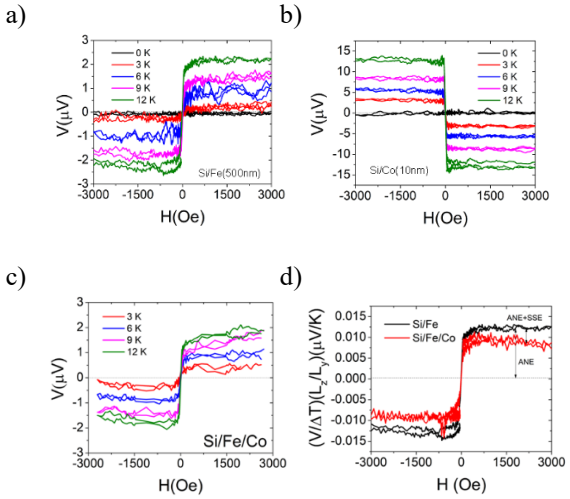

Fig.12 The magnetic field ***(H)*** dependence **a)** Fe*(*500nm*)* **b)** Co*(*10nm*)* **c)** Fe*(*500nm*)*/Co*(*10nm*)* **d)** The normalized voltage ***(E ∇T)*** of Fe*(*500*)* and Fe*(*500*)*/Co*(*10*)*

IV. CONCLUSION

This research explores the structural properties of Fe/Co and Co/Pt systems, comparing them to the Fe/Pt system structure through Density Functional Theory (DFT) calculations. It shows that the electrical mismatches in the Fe/Co and Co/Pt structures are significantly smaller than in the Fe/Pt system, as seen from the Total Density of States (TDOS) near the Fermi energy level. This suggests a preference for selecting materials to study the Spin Seebeck Effect (SSE). Additionally, the Projected Density of States (PDOS) for the Fe and Co structures in the Fe/Co system, and the PDOS for the Co and Pt structures in the Co/Pt system, indicate that the main features of both systems come from the d orbitals. These computational results help in pre-examining the electronic properties of materials before experimental studies on the Spin Seebeck Effect (SSE), including their electrical conductivity and magnetic properties.

ACKNOWLEDGMENT

The researcher would like to express gratitude to the Synchrotron Light Research Institute (Public Organization) for providing the resources to use the VASP (Vienna Ab initio Simulation Package) for mathematical simulation calculations, and would like to thank the scholarship from the Quantum Technology Research and Development Group, Department of Electrical and Computer Engineering, Thammasat School of Engineering, Thammasat University.

REFERENCES

[1] H. Adachi, K. Uchida, E. Saitoh, and S. Maekawa, "Theory of the Spin Seebeck Effect," Reports on Progress in Physics, vol. 76, no. 3, p. 036501, 2013.

[2] K. Uchida, J. Xiao, H. Adachi, J. Ohe, S. Takahashi, J. Ieda, ... E. Saitoh, "Spin Seebeck insulator," Nature Materials, vol. 9, no. 11, pp. 894-897, 2010..

[3] G. E. W. Bauer, E. Saitoh, and B. J. van Wees, "Spin caloritronics," Nature Materials, vol. 11, no. 5, pp. 391-399, 2012, DOI: 10.1038/nmat3301.

[4] H. Adachi, K. Uchida, E. Saitoh, and S. Maekawa, "Theory of the Spin Seebeck Effect," Physical Review B, vol. 88, no. 9, 094403, 2013, DOI: 10.1103/PhysRevB.88.094403.

[5] S. R. Boona, R. C. Myers, and J. P. Heremans, "Spin caloritronics," Energy & Environmental Science, vol. 7, no. 3, pp. 885-910, 2014, DOI: 10.1039/c3ee43299h.

[6] G. Kresse and J. Furthmüller, "Efficiency of ab-initio total energy calculations for metals and semiconductors using a plane-wave basis set," Computational Materials Science, vol. 6, no. 1, pp. 15-50, 1996.

[7] V. Kalappattil, R. Geng, R. Das, M. Pham, H. Luong, T. Nguyen, A. Popescu, L. M. Woods, M. Kläui, H. Srikanth, and M. H. Phan, "Giant Spin Seebeck Effect through an Interface Organic Semiconductor," Materials Horizons, pp. 1413-1420, 2020.

[8] C. Horprathum, C. Chananonnawathorn, P. Piyasind, S. Pinitsoontorn, H. Ramamoorthy, R. Somphonsane, W. Pijitrojana, S. Ummartyotin, P. Kalasuwan, and P. Wongjoma, "Investigating the shunting effect in a Fe/Co ferromagnetic metal hybrid structure and its impact on the spin Seebeck effect," Physical Review B, 2024, in the process of publishing.

[9] Bavontaweepanya R, Infahsaeng Y, Pongophas E, Maiaugree W, Piyasin P, Palaporn D, et al. The observation of spin Seebeck effect in opposite spin Hall angle materials of polycrystalline bulk-Fe3O4/(Co/Fe) systems. AIP Adv. 2022;12(1):015320.